Determination of the dynamic elastic properties of paper and paperboard from the low-frequency vibration modes of rectangular plates

JUN SATO[1], IAN M. HUTCHINGS[2] AND JIM WOODHOUSE[3]

SUMMARY

The dynamic elastic constants of paper/paperboards are determined by using the vibrational resonance modes. The vibration modes can be visualised by Chladni figures and correspond to the eigen-frequencies of the plates. The values of Young's modulus derived by this method are lower than those obtained from ultrasonic measurements at higher frequencies, which is consistent with a viscoelastic behaviour in which elastic modulus depends on frequency. The in-plane shear modulus and dynamic Poisson's ratios in the MD and CD can also be derived with high reproducibility. In order to determine these elastic constants it is usually necessary to observe five low-frequency vibration modes, but it has been shown that only three modes are needed if the shapes of the nodal lines in the Chladni patterns are also taken into consideration. A simpler method is also suggested as a practical approach which also gives consistent results with other methods.

KEYWORDS

paperboard, vibration, elastic modulus, Poisson's ratio, Chladni pattern, nodal line

INTRODUCTION

The methods most commonly used to determine the elastic modulus of paper or paperboard are tensile testing (i.e. a quasi-static method) and ultrasonic methods (dynamic methods) (e.g. Habeger (*1*)). Some of the latter methods use a pulsed laser to generate an ultrasonic signal without physical contact (Brodeur et al. (*2*), Scruby and Drain (*3*)). However, these methods do not explore the elastic properties in the audio frequency range which is important in the actual paper-converting process. For instance, paper tubes used in the textile or film industries rotate with frequencies from a few Hz to 300 Hz, much lower than the frequencies of 50-100 kHz commonly used in ultrasonic measurements.

Because the elastic constants of paper vary with vibrational frequency, it is important to know their accurate values under conditions appropriate to practical applications. A method involving forced vibrations of reeds (Horio and Onogi (*4*), Sakmen and Hagen (*5*)) has been used to determine the elastic modulus of films at low frequency, and has also been applied to paper strips, although it is now rarely employed in the paper industry. Like the reed vibration method, the vibration method described below also utilises eigen-frequencies for out-of-plane vibration of a sheet. However, there is no need to clamp the paper strip nor to change its direction; it is also possible to derive values for the dynamic Poisson's ratios and shear modulus. The sample sheets used in this method are wide rectangles or squares rather than narrow strips.

The frequency range used in the present method is 10 to 1000 Hz, much lower than that used in the ultrasonic methods. In order to visually identify the resonance of the sheet, Chladni patterns are used. The German physicist Ernst Chladni (1756-1827) performed classical experiments to study the effects of harmonic vibrations in elastic plates (Soedel (*6*)). He spread fine sand on to the plate and set it into vibration by scraping a violin bow along one edge. The vibrating plate forms standing waves at an eigen-frequency, with a distribution of nodal and anti-nodal regions. The fine particles move from the anti-nodes towards the nodal lines, forming symmetrical patterns called Chladni patterns. There are an infinite number of Chladni patterns, corresponding to the infinite number of vibrational modes. The present method, however, uses only a few low-frequency modes as shown in Figure 1, and they are excited by a loudspeaker rather than by a violin bow.

Chladni patterns can be observed on plates of a wide range of materials such as glass, metals, ceramics, wood, composite materials, laminated board, corrugated board (Lu and Zhu (*7*)), and rocks. The patterns become more complicated at higher frequencies, even providing inspiration for some artists.

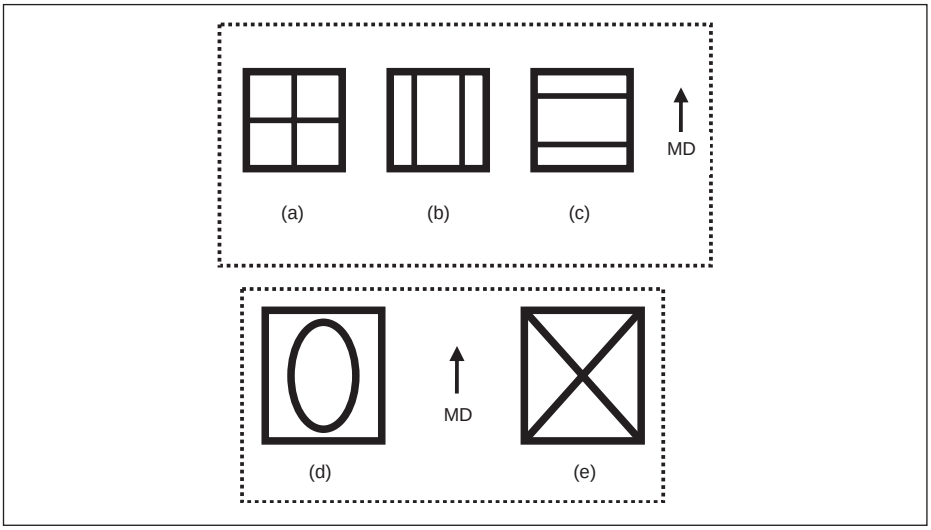

Fig 1. Schematic diagrams showing the low-frequency modes of Chladni patterns for square and rectangular plates: (a) + mode; (b) bending mode (CD : Cross direction); (c) bending mode (MD :Machine Direction); (d) Ring-mode; (e) X-mode.

[1]Visiting Scientist and Corresponding author (junsato@marutsutsu.co.jp), [2]Professor
Institute for Manufacturing
University of Cambridge
Mill Lane, Cambridge CB2 1RX, UK
[3]Professor
Department of Engineering
University of Cambridge
Trumpington Street, Cambridge, CB2 1PZ, UK

THEORETICAL BACKGROUND

The theory used here is mainly based on the work of McIntyre and Woodhouse (*8*). First we assume that machine-made paper can be treated as a thin, flat orthotropic plate. The bending vibration of such a plate is governed by four elastic constants. If a sinusoidal acoustic wave is applied perpendicularly to the plate surface the out-of-plane displacement w can be expressed as $w(x,y)e^{iwt}$. For a free-edged plate A (length a and width b) of small thickness h lying in the x-y plane, the potential energy function is given by:

$$P = \frac{h^3}{2}\iint \left[\begin{array}{l} D_1\left(\frac{\partial^2 w}{\partial x^2}\right)^2 + D_2\frac{\partial^2 w}{\partial x^2}\frac{\partial^2 w}{\partial y^2} + \\ D_3\left(\frac{\partial^2 w}{\partial y^2}\right)^2 + D_4\left(\frac{\partial^2 w}{\partial x \partial y}\right)^2 \end{array} \right] dA \qquad [1]$$

where the double integral is taken over the plate area and D_1,D_2,D_3 and D_4 are bending stiffness normalised by h^3.

The kinetic energy function for angular frequency ω is written as follows:

$$K = \frac{1}{2}\rho h\omega^2 \iint w^2 dA \qquad [2]$$

where ρ is the density of the plate.

When the plate is in a vibration mode, Rayleigh's principle yields the eigen-frequency as follows, by combining eqs. [1] and [2] to give;

$$\omega^2 = \frac{h^2 \iint \left[\begin{array}{l} D_1\left(\frac{\partial^2 w}{\partial x^2}\right)^2 + D_2\frac{\partial^2 w}{\partial x^2}\frac{\partial^2 w}{\partial y^2} + \\ D_3\left(\frac{\partial^2 w}{\partial y^2}\right)^2 + D_4\left(\frac{\partial^2 w}{\partial x \partial y}\right)^2 \end{array} \right] dA}{\rho \iint w^2 dA} \qquad [3]$$

The four elastic constants D_1, D_2, D_3 and D_4 can be written in terms of Young's modulus E, Poisson's ratio and the shear modulus G_{xy} as follows :

$$D_1 = E_x/12\mu, \quad D_2 = \nu_{xy}E_y/6\mu = \nu_{xy}E_x/6\mu$$

$$D_3 = E_y/12\mu, \quad D_4 = G_{xy}/3 \qquad [4]$$

where $\mu = 1-\nu_{xy}\nu_{yx}$.

The vibration modes give rise to Chladni patterns corresponding to each resonant frequency. The modes used in this method are as follows:

(a) + mode (twisting mode) : freq. f_+
(b) Bending mode in CD : freq. f_{b1}
(c) Bending mode in MD : freq. f_{b2}
(d) Ring-mode: freq. f_o
(e) X-mode : freq. f_x

For the + mode, it has been shown that $w(x,y) = xy$ gives a good approximation (Leissa (*9*), Rayleigh (*10*)). Therefore eq.[3] yields

$$D_4 \approx 0.274 f_+^2 \rho a^2 b^2 / h^2 \qquad [5]$$

The modes (b) and (c) (Fig. 1) are bending modes and are well approximated by the one-dimensional bending motion of a bar. Therefore these can be written as:

$$D_1 \approx 0.0789 f_{b1}^2 \rho a^4 / h^2 \qquad [6]$$

and

$$D_3 \approx 0.0789 f_{b2}^2 \rho b^4 / h^2 \qquad [7]$$

D_2 is calculated by observing (d) the Ring-mode and (e) the X-mode. These two modes are excited only when the aspect ratio of the sample plate is adjusted as follows:

$$\frac{a_{ox}}{b_{ox}} = \left(\frac{D_1}{D_3}\right)^{\frac{1}{4}} \qquad [8]$$

If a square sample is used to determine D_1, D_2 and D_3, eq.[8] can be written in simpler form as:

$$\frac{a_{ox}}{b_{ox}} = \left(\frac{f_{b1}}{f_{b2}}\right)^{\frac{1}{2}} \qquad [9]$$

For a square sheet, the excited mode splits into the Ring-mode and X-mode due only to Poisson coupling, without which these two modes become degenerate. Observation of the Ring and X modes can provide information about the Poisson's ratios in the x and y directions. After adjusting the aspect ratio of the sample the two resonance frequencies for the Ring-mode (f_o) and X-mode (f_x) are measured and D_2 is estimated from these two frequencies by:

$$D_2 \approx 0.114(f_o^2 - f_x^2)\rho a^2 b^2 / h^2 \qquad [10]$$

In this way we can obtain approximate values for the four bending stiffnesses D_1-D_4, and the Young's modulus, the shear modulus and Poisson's ratios are obtained from eq.[4]. However we should note that the eigen-frequency derived by Rayleigh's principle is always higher than the actual value. McIntyre and Woodhouse (*8*) employed the Rayleigh-Ritz method in order to get more precise results. In the iterative process, the values of D_1-D_4 given by eqs. [5], [6], [7] and [10] are adopted as initial values, from which we can calculate eigen-frequencies for each mode by eq.[3]. Minimising the difference between measured and predicted frequencies leads to more precise results. In an iterative program employing the Rayleigh-Ritz method, the trial function used was

$$w(x,y) = \sum_{n=1}^{N}\sum_{m=1}^{M} a_{nm} x^n y^m \qquad [11]$$

One can thus determine the unknown coefficients a_{nm} and can start the iteration, the convergence of which is confirmed by McIntyre and Woodhouse (*8*). It is also noted that the free boundary condition is essentially taken into account as a kind of 'natural' boundary condition.

MATERIALS AND EXPERIMENTAL METHODS

Various samples of Japanese paperboard were tested to measure their elastic constants at audio frequencies (Sato et al. (*11*)). Most of these samples are used as core-board for paper tubes.

Sample preparation

The paperboard samples (No.1 - -No.12) with various thickness (0.6mm, 0.7mm, 0.8mm, and 1.0mm) were kept under standard ambient condition (20°C, 65% RH) before the experiments. Samples were precisely cut parallel to MD and CD into rectangular and square shapes. In most cases squares were used because the elastic constants of machine-made paper are sufficiently different in the x and y directions to excite two bending modes with different frequencies. If the material were isotropic then these two bending modes would be degenerate.

The sample mass and thickness were carefully measured. In principle there is no restriction in sample size, but the sheet must be sufficiently flat during the measurements. The samples of core-board with a thickness of. 0.5 to 1.0 mm were typically 100 to 150 mm square.

Experimental procedure

The experimental system is shown schematically in Figure 2. A loudspeaker driven by a sine-wave generator and amplifier is mounted beneath a hole 20 to 50 mm in diameter in a large flat surface. The frequency is monitored with a digital frequency counter. The sample is support-

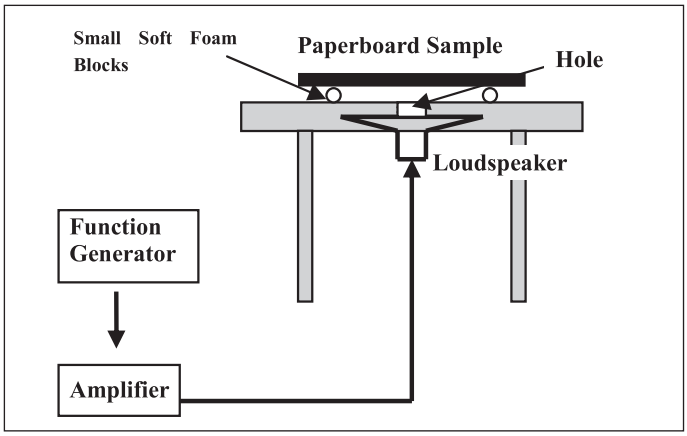

Fig. 2 Schematic diagram of the measurement system .

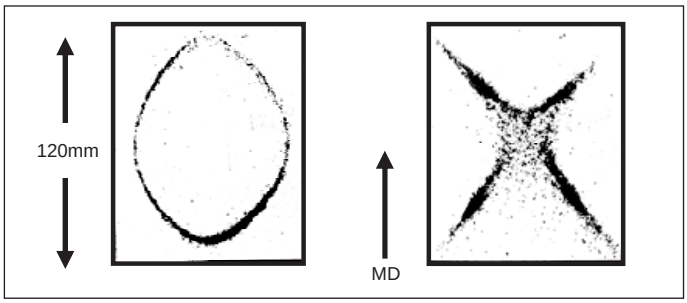

Fig. 4 Examples of Ring-mode and X-mode patterns observed after re-sizing of a core-board sample.

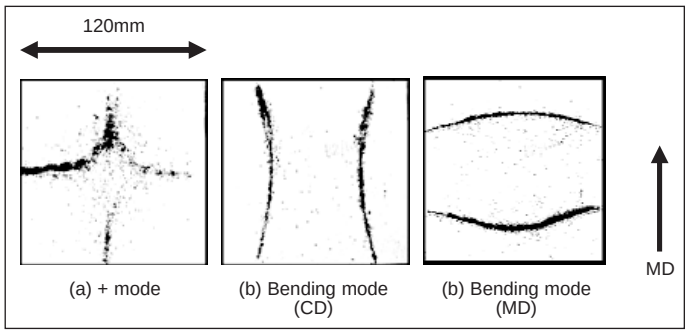

Fig. 3 Photographic images showing three low-frequency modes for a core-board sample (120 x 120 x 0.8 mm).

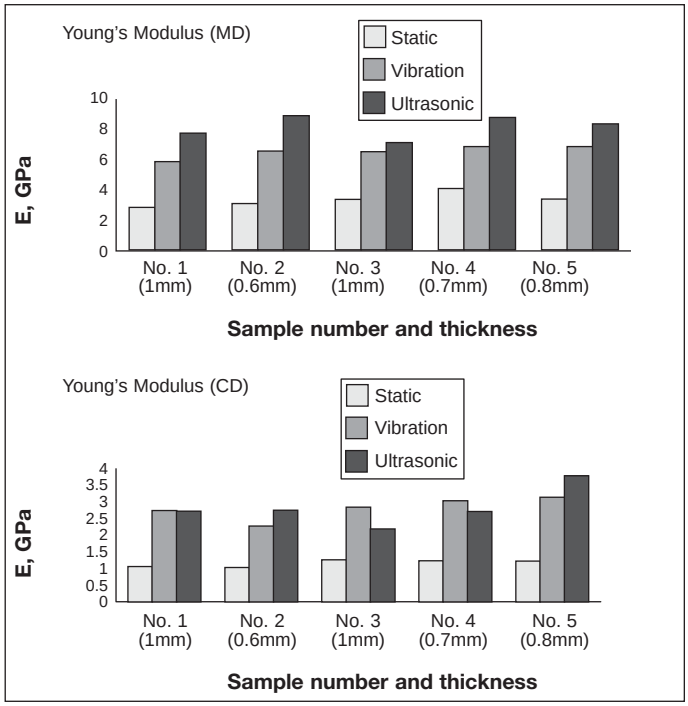

Fig. 5 Young's modulus of the core-board samples in MD and CD determined by the three different methods.

ed above the hole by four or five small pieces of plastic foam whose positions are carefully set beneath the expected nodal lines of each vibration mode, so that the supports do not affect the boundary conditions. The sample is placed so that an anti-nodal area faces the loudspeaker hole.

Fine particles such as sand or tea leaves are sprinkled over the sample in order to visualise the Chladni patterns. Careful tuning of frequency and power is needed to excite each vibration mode, which is identified when the particles cluster on the nodal lines. Figure 3 shows images of typical low-frequency Chladni patterns on a core-board sample.

The excitation frequencies for the first three low-frequency modes are measured. The plate is then carefully re-sized according to eq. [8] or eq. [9], and the Ring-mode and X-mode are excited. The elastic constants are calculated by use of the theory described in the previous section. Figure 4 shows examples of Ring-mode and X-mode patterns obtained after adjusting the aspect ratio of a core-board sample, as used for the images in Figure 3.

RESULTS AND DISCUSSION

As mentioned above there are several methods to determine the elastic constants of paper. The results of the present plate-vibration method have been compared with those from other methods.

Comparison of Young's modulus by three different methods

The tensile testing and ultrasonic methods were both employed for comparison with the vibration method. The samples were held at 23°C and 50% RH before the measurements. The tensile testing procedure was based on the Japanese Industrial Standard method (JIS P8113). The quasi-static Young's modulus was obtained from the stress-strain curve. In the ultrasonic measurement, commercial equipment (SST 200, Nomura Shoji Co. Ltd.) was employed. The frequency of the source was 25 kHz and the distance between the two transducers was fixed at 150 mm. The sample was placed on a disc-shaped foam rubber support (10 mm thick). After measurement of the velocities in the *x* and *y*-directions, the Young's modulus was calculated from the following equations:

$$E_x = \rho c_x^2 \mu \text{ and } E_y = \rho c_y^2 \mu \qquad [12]$$

where μ=1-$v_{xy}v_{yx}$ and c is the velocity of the longitudinal wave. It should be noted that one cannot obtain the Poisson's ratios v_{xy} and v_{yx} only from velocity measurement of the longitudinal wave, and therefore the two values of dynamic Poisson's ratio derived by the vibration method were used in eq. [12].

The Young's moduli from the three different methods (Static, Vibration and Ultrasonic) for MD and CD are compared in Figure 5. These five paperboard samples are different grades and made from different raw materials. Therefore it would be reasonable for their viscoelastic properties to be different. The vibration

Table 1
Ratios between dynamic and static Young's modulus in MD and CD

	MD : *E*(Vib)/*E*(St)	CD : *E*(Vib)/*E*(St)
No.1 (1.0mm)	2.1	2.7
No.2 (0.6mm)	2.2	2.3
No.3 (1.0mm)	2.0	2.0
No.4 (0.7mm)	1.7	2.5
No.5 (0.8mm)	2.1	2.7

method gives relatively smaller values compared with the ultrasonic method, but much larger than the static values. Paper is a viscoelastic material and its elastic properties are thought to be frequency-dependent. At higher frequencies there is not enough time for stress relaxation, which results in a higher elastic modulus. The results obtained here are consistent with this.

The ratios between the dynamic and static Young's modulus (*E*(vib)/*E*(st)) are different in MD and CD, where *E*(vib) is the value of Young's modulus determined by the vibration method and *E*(st) is by the static method. Table 1 summarises the results.

Besides the fact that the values of *E*(vib) are always higher than *E*(st) for both directions, the ratios *E*(vib)/*E*(st) are larger in CD direction than MD. This result supports the suggestion that properties along CD are more sensitive to frequency change (Habeger (*1*)), essentially due to the anisotropic change in the viscosity of paper (Kadoya et al (*12*)), although there are other interpretations (Habeger (*1*), Zauscher (*13*)). Along the MD the mechanical properties are mainly governed by the cellulose fibres themselves, while the amorphous polymeric behaviour becomes more significant along the CD as the deformation of the linkage between the fibres plays a more important role in this orientation.

Sample size and excitation frequency

Generally the excitation frequency rises as the sample becomes smaller. If the Young's modulus were very sensitive to frequency in the range used in these experiments (10 to 1000Hz) it might be possible that the sample size would affect the measured values of Young's modulus. A series of tests was therefore performed in which the sizes of the samples were changed from 75 x 75 mm to 150 x 150mm. Table 2 shows some results from these tests.

Over this frequency range (44 to 157 Hz), no significant changes were observed for the different sample sizes, which leaves the experimenter with some freedom to choose the optimum size. The dynamic Poisson's ratios are also listed in the table. These values are highly consistent with the results obtained by bi-axial tensile testing or other type of ultrasonic measurement (Hardecker (*14*), Baum (*15*)).

Table 2:
Elastic constants determined for samples of the same core-board with different sizes. Thickness was 0.6 mm and the plates were square

No.7 (t=0.6mm)	size (mm)			
	150 x 150	120 x 120	100 x 100	75 x 75
Frequency for 1st mode (Hz)	44	56	93	157
E(MD) in GPa	6.1	6.5	6.5	6.6
E(CD) in GPa	2.6	2.3	2.2	2.3
Poisson's Ratio (MD)	0.37	0.38	0.38	0.38
Poisson's Ratio (CD)	0.16	0.14	0.13	0.13

Effect caused by defects in paper

Paper is an imperfect material and normally has local inhomogeneity such as fibre flocks or damaged regions. A sample with such defects will have different mechanical properties from a more perfect sample, including variability in strength and stiffness. For this reason it is desirable to use a test method which can detect and reflect such effects in the results. Ultrasonic methods, however, are not sensitive to these kinds of defects unless they are located on the line between the two transducers. Experiments were performed to establish whether the effects of local defects are reflected in the resonance frequencies or Young's modulus derived by the vibration method. Artificial defects in the form of four small surface regions (four circular areas of radius 15 mm) were scratched on the sample with a sharp needle, as shown in Figure 6.

It is not easy to quantify such scratched grooves accurately, but by using an optical profilometer each groove was found to be 50 to 100 μm deep and 50 to 100 μm wide. Ten scratches were made parallel to the MD and the CD in a grid formation in each area. The experiment was repeated five times, with more scratches being added each time, and the changes in excitation frequencies and Young's modulus were determined.

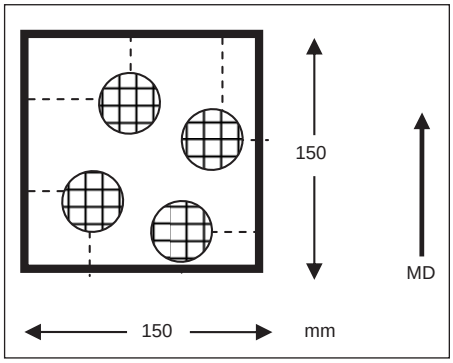

Fig. 6 Diagram showing the four circular areas on the paperboard surface where scratches were made in a grid-pattern.

Table 3 shows the results. The resonant frequencies, and the elastic moduli derived from them, became lower as the extent of surface damage was increased. The values of Young's modulus determined by the vibration method are clearly sensitive to the surface defects in the samples.

Shapes of the nodal lines

The curvatures of the nodal lines in the two bending modes are different for different materials or for rectangular plates

Table 3.
Changes in Young's modulus and excitation frequencies due to progressive surface damage, showing values for the undamaged paperboard and samples with from one to five cycles of scratch damage.

	Undamaged	1 Damage Cycle	2 Damage Cycles	3 Damage Cycles	4 Damage Cycles	5 Damage Cycles
E(MD) GPa	6.93	6.70	6.44	6.35	6.07	5.75
E(CD) GPa	3.48	3.30	3.29	3.13	3.18	2.97
Freq. + Mode (Hz)	62	60	60	57	56.5	53
CD Bend. Mode (Hz)	77	75	74.8	73	73.5	71
MD Bend. Mode (Hz)	114	112	110	109	107	104

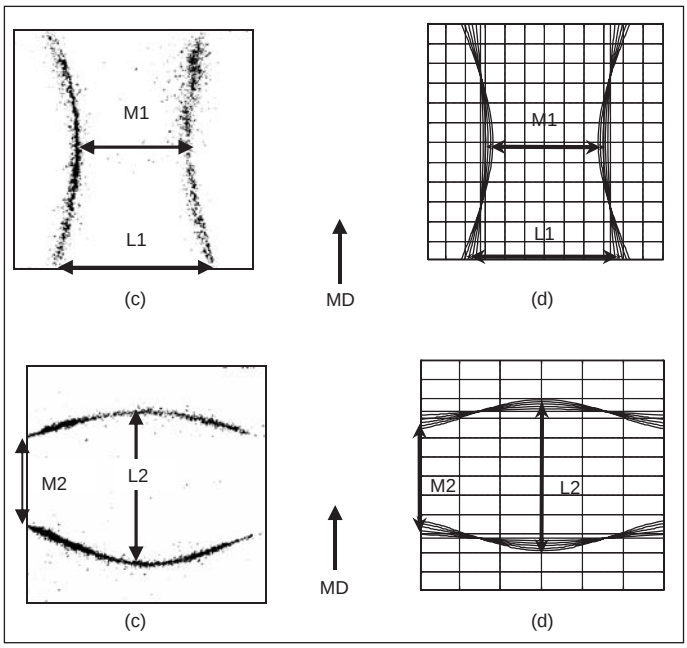

Fig 7: The nodal lines for the two bending modes of a paperboard sample; (a) and (c) observed, and (b) and (d) calculated figures for different Poisson's ratios. Sample size was 120 x 120 x 0.8 mm.

Table 4
Comparison between elastic constants determined by method A and method B; method A uses Ring-mode and X-mode resonance, while method B uses the curvature of the nodal lines of the bending modes. The figures in brackets are sheet thicknesses in mm.

	Young's Modulus in GPa		Poisson's Ratio		Shear Mod. in GPa
	E (MD)	*E (CD)*	ν_{xy}	ν_{yx}	G_{xy}
Lami. B. (3.0)					
method A	1.55	0.56	0.36	0.13	0.34
method B	1.58	0.56	0.29	0.10	0.34
No.1 (1.1)					
method A	5.93	2.52	0.42	0.18	1.32
method B	5.94	2.52	0.45	0.20	1.32
No.5 (0.8)					
method A	6.90	2.91	0.37	0.16	1.61
method B	7.12	2.89	0.27	0.11	1.61
No. 7 (0.6)					
method A	8.83	2.61	0.21	0.06	1.91
method B	8.87	2.61	0.19	0.06	1.91
No. 8 (0.6)					
method A	9.63	3.10	0.36	0.12	1.86
method B	9.90	3.10	0.19	0.06	1.85
Steel (SUS304)					
REF. Value	197	197	0.31	0.31	75
method B	199	205	0.30	0.31	68
Aluminium					
REF. Value	70	70	0.35	0.35	26
method B	68	64	0.35	0.33	26

with different aspect ratio (Fletcher et al. (*16*)). In fact, the shapes of the nodal lines contain information about Poisson's ratio for the material. The nodal line is the locus of points which satisfy the equation $w(x,y,t) = 0$ and is visualised since this is where the particles collect at resonance. The vibrating plate shows anticlastic bending because of Poisson coupling, and the nodal lines are not straight as they would be for flexural bending of a narrow beam. The curvature of the lines seen on a square plate depends on the value of Poisson's ratio and the ratio between E(MD) and E(CD). The nodal line becomes more curved for higher Poisson's ratio and a lower ratio of E(MD)/E(CD).

Figure 7 shows an example of the nodal lines of the two bending modes in MD and CD. Figure 7(a) and (c) show the Chladni figures for a core-board sample (No.3 in Fig. 5). Figures 7(b) and (d) show calculated nodal line shapes for five different values of Poisson's ratio (ν_{xy}=0.1, 0.2, 0.3, 0.4 and 0.5). The curvature of the line increases as Poisson's ratio approaches 0.5. The line is straight if the Poisson's ratio is zero. Measurements of the ratios L1/M1 and L2/M2 can be used to identify the value of Poisson's ratio which gives the best fit to the experimental curves.

Fitting two Chladni patterns provides an alternative way to determine the elastic constants. We will call this 'method B', while the previous method is called 'method A'. In method B the Ring-mode and X-mode are not required and therefore one does not need to adjust the aspect ratio of the plate, which is often beneficial.

The experimental procedure is as follows:

1. Measure the frequencies of the three modes which are shown in Figure 1 (a), (b) and (c) and calculate the estimated values of D_1, D_3 and D_4 using eqs. [5],[6] and [7]
2. The nodal lines (Chladni figures) for the two bending modes are compared with the shapes predicted for a range of values of Poisson's ratio (which relates to D_2). Find the values of Poisson's ratio for which the nodal lines best fit the predicted curves. The ratios M1/L1 and M2/L2 can be used for this.
3. Once an estimated value of D_2 is obtained, the Young's modulus and Poisson's ratios are derived as in method A.

Table 4 shows the results obtained by this method compared with those from the method using the Ring-mode and X-mode. Results from these methods are in reasonable agreement for the five types of paperboard. Sheets of steel and aluminium alloy, assumed to be isotropic and with well-defined elastic constants, were also tested to verify the accuracy of the methods. The results are in good agreement with the reference values (National Astronomical Observatory (*17*)). It is therefore proposed that one can derive both Young's modulus and the Poisson's ratios in the x and y directions by utilising the information from Chladni patterns.

Simple method for paperboard

As shown above, one can determine the Young's modulus and the Poisson's ratio by either method A or method B, and these methods give consistent results. However a simpler method can also be useful to make a quick estimate of the Young's modulus for samples of a single class of material such as paper or paper-

board, between which there is little practical variation in Poisson's ratio. For example, for regular paperboard the value of $\mu = 1\text{-}\nu_{xy}\nu_{yx}$ is found to fall in the range of 0.90 to 0.95. The dynamic Poisson's ratios of liner board are 0.35 to 0.50 and 0.15 to 0.20 in each direction (Baum and Bornhoeft (*15*)) giving a value of μ of about 0.93. In this case D_2 can be written as follows from eq. [4];

$$D_2 = 2\left(\nu_{xy}\,\nu_{yx} D_1 D_3\right)^{\frac{1}{2}} \approx 0.53\left(D_1 D_3\right)^{\frac{1}{2}} \qquad [13]$$

This can be used as a starting value for the iterative program used in method A. As shown in Table 5, the results determined by this simple method (method C) are quite close to those obtained by method A. For some purposes, it may be adequate to use method C.

The Poisson's ratios in Tables 4 and 5 may appear to be lower than the values determined by biaxial testing. However the Poisson's ratios derived by our vibration method are dynamic values which are likely to be smaller than static values due to the viscoelastic nature of paper. The dynamic Poisson's ratios measured by ultrasonic testing are often even smaller (Baum and Bornhoeft (*15*)).

Vibration method and ultrasonic method

The relationship $E = \rho c^2$ is commonly used to obtain Young's modulus from a measurement of sound velocity. However, this equation applies to longitudinal waves propagating in a thin bar whose diameter is smaller than the wavelength. In this case a diametral Poisson strain can occur, whereas for longitudinal wave propagation in a paperboard sheet as used in the ultrasonic methods, the in-plane Poisson strain must be zero. The stress component in the *z*-direction (out-of-plane) must also be zero. In this case the Young's modulus in the *x* and *y* directions should be determined from eq.[12], where c_x and c_y are the velocities of longitudinal waves in the *x* and *y* direction respectively.

When the sample contains defects of some kind, ultrasonic testing may lead to misleading results unless the defects are located on the path between the transmitter and receiver, because only the travel time of the primary wave is measured. In the vibration method, on the other hand, the whole sample vibrates and the excitation frequency for each mode decreases according to the damage level. The effects of defects are more likely to be reflected in the elastic modulus, as shown in Table 3. It should be also noted that the ultrasonic method will always give the higher elastic modulus as the primary wave propagates along the fastest path near the measurement line. Properties determined by the vibration method can reflect those of the weaker part of the sample, which is an advantage when considering the properties of paper under tensile loading.

Table 5
Comparison of results from method A and method C (simple method).

	Young's Modulus in GPa		Poisson's Ratio	
	E (MD)	*E (CD)*	ν_{xy}	ν_{yx}
No. 9 (0.6)				
method A	7.33	2.83	0.43	0.17
method C	7.37	2.87	0.41	0.16
No.10 (0.7)				
method A	6.07	2.46	0.37	0.15
method C	6.10	2.40	0.39	0.15
No.11 (0.8)				
method A	7.91	2.98	0.35	0.13
method C	7.88	2.99	0.36	0.14
No. 12 (1.0)				
method A	6.66	2.70	0.42	0.17
method C	6.60	2.62	0.40	0.06

CONCLUSIONS

It has been shown that a vibration method involving the visualisation of standing acoustic waves on the surface of a sheet can be used to determine values of dynamic Young's modulus and Poisson's ratios for orthotropic paperboards with good accuracy. The Young's modulus values determined in this way were lower than those measured by ultrasonic methods and higher than those measured by quasi-static tensile testing, which is consistent with viscoelastic behaviour in which the elastic modulus depends on frequency.

In comparison with the commonly-used ultrasonic method which also gives the dynamic Young's modulus, the vibrational method has several advantages including speed, stability and simplicity of the measurements, easy derivation of the Poisson's ratios and shear modulus, reflecting the whole sheet properties rather than the local inhomogeneity. It also simulates the elastic properties in a more industrially-relevant frequency range. The vibration method is well suited for non-uniform and imperfect sheet materials such as paper and paperboard. There is no particular restriction to the sample size as long as it is kept flat during the measurement. (The method could in principle be applied to an even smaller size such as a postage stamp.) The shapes of the nodal lines of the vibrational modes (Chladni figures) contain useful information on the elastic properties of the material: the curvatures of the nodal lines can be used to determine Poisson's ratio.

REFERENCES

(*1*) Habeger Jr. C.C. – Ultrasonic determinations of paper stiffness parameters, In Mark RE et al. (ed.) **Handbook of Physical Testing of Paper**, Marcel Dekker, NY, p.257 (2002).

(*2*) Brodeur P.H. et al. – Noncontact laser generation and detection of Lamb waves in paper, *J. Pulp Paper Sci.*, **23**(5):J238 (1997).

(*3*) Scruby C.B. and Drain L.E. - **Laser Ultrasonics**, Taylor & Francis Group, NY, p.356 (1990).

(*4*) Horio M. and Onogi S. – Forced vibration of reed as a method of determining viscoelasticity, *J. Appl. Phys.*, **22**(7):977 (1951).

(*5*) Sakmen H. and Hagen R. –Viscoelastic properties, In Mark RE et al. (ed.) **Handbook of Physical Testing of Paper**, Marcel Dekker, NY, p.77 (2002).

(*6*) Soedel W. – **Vibrations of Shells and Plates**, Marcel Dekker, NY, p.3 (2004).

(*7*) Lu T.J. and Zhu G. – The elastic constants of corrugated board panels, *J. Composite Materials*, **35**(20):1868 (2001).

(*8*) McIntyre M.E. and Woodhouse J. – On measuring the elastic and damping constants of orthotropic sheet materials, *Acta Metall.*, **36**(6):1397 (1988).

(*9*) Leissa A.W. – **The Vibration of Plates**, NASA SP-160, Washington D.C., p.92 (1969).

(*10*) Rayleigh J.W.S. – **The Theory of Sound**, Dover, NY, p.372 (1945).

(*11*) Sato J. et al. – Measurement of the elastic modulus of paperboard from the low-frequency vibration modes of rectangular plates, *Jpn. Tappi J.* **61**(7):71 (2007).

(*12*) Kadoya T. et al. – **Shin Kami no Kagaku** (Japanese) : Chugai-sangyo Chousakai , Tokyo, p.330 (1989).

(*13*) Zauscher. et al. – The influence of water on the elastic modulus of paper, *Tappi J.*, **79**(12):178 (1996).

(*14*) Hardecker K.W. – Instrument and specimen shape for biaxial testing of paper, *J.Phys. E.*, 14:593 (1981).

(*15*) Baum G.A. and Bornhoeft L.R. – Estimating Poisson ratios in paper using ultrasonic techniques, *IPC Technical Paper Series*, 69:1 (1978).

(*16*) Fletcher N.H. et al. – **Gakki no butsurigaku** (Japanese version of 'The Physics of musical instruments'), Springer Japan, Tokyo, p.80 (2002).

(*17*) National Astronomical Observatory (ed.) – **Chronological Scientific**, Maruzen, Tokyo, p.375 (2005).

Original manuscript received 27 June 2007, revision accepted 8 November 2007